A 3-D finite element model for thermal analysis of laser assisted fiber placement

Celik, Ozan; Shroff, Sonell; Teuwen, Julie; Bergsma, Otto; Benedictus, Rinze

Publication date
2018

Document Version
Accepted author manuscript

Published in
Proceedings of the SAMPE Europe Conference 2018 Southampton

A 3-D FINITE ELEMENT MODEL FOR THERMAL ANALYSIS OF LASER ASSISTED FIBER PLACEMENT

Ozan Çelik[1], Sonell Shroff, Julie J. E. Teuwen, Otto K. Bergsma, Rinze Benedictus
Delft University of Technology, Structural Integrity and Composites Department
Kluyverweg 1, Delft, 2629 HS, The Netherlands

[1]Corresponding author. E-mail: ozan.celik@tudelft.nl

ABSTRACT

Laser assisted automated tape or fiber placement (LATP/LAFP) with in-situ consolidation is a promising technique for manufacturing large structures, eliminating the limitations of autoclave curing. Currently, 2-D models are mostly preferred for the thermal analysis of the process. A 3-D, transient thermal finite element model is developed to analyze the effect of the alignment of the heat source with the tape laying direction and is compared with a model imitating a 2-D analysis space. This aspect of the process has not been considered in the literature so far. Effects of this aspect on temperature history and intimate contact evolution are presented.

1. INTRODUCTION

Larger structures are becoming available to be produced with the LAFP process thanks to the experience gained in this field in the last few decades. As the dimensions and the complexity of the tape placed structures increase, new design features such as fiber steering for optimized structure performance [1] emerge. Predicting the final quality of the manufactured parts containing these type of design features is a new challenge.

Thermal history during the tape placement process has been of primary interest in process control due to its close link to the quality aspects of the final product such as interlaminar bonding, crystallinity, void content and residual stresses. 2-dimensional models considering the length and thickness directions of the thermal analysis of LAFP have been very common in the literature [2]. This approach is mostly preferred due to its computational simplicity. However, such an analysis scheme would omit the in-plane conductivity of the material and thermal/optical interactions as a result of fiber orientation difference between the tape and the substrate. The effects of these aspects on the temperature predictions has not been deeply investigated.

In this work, the validity of a 2-D modeling space to analyze the thermal phenomena during the tape placement of a multi-axial laminate is investigated. This is done by analyzing a 3-D model of the tape placement process with two different heat source movement schemes. In the first one, the heat source moves along the incoming tape direction for each layer, while the second one moves in the direction of the first placed layer through the whole process, regardless of the actual tape placement orientation. The latter one is an imitation of the 2-dimensional analysis domain.

2. THE PROCESS FINITE ELEMENT MODEL

2.1 Process Model

The LAFP process is schematically shown in Figure 1. The dynamic nature of heating and cooling requires the tape, substrate, heat source and losses to the environment to be modelled. ABAQUS finite element package is used for the transient heat transfer analysis. DC3D8 heat transfer brick elements are used for modelling the tape and the substrate.

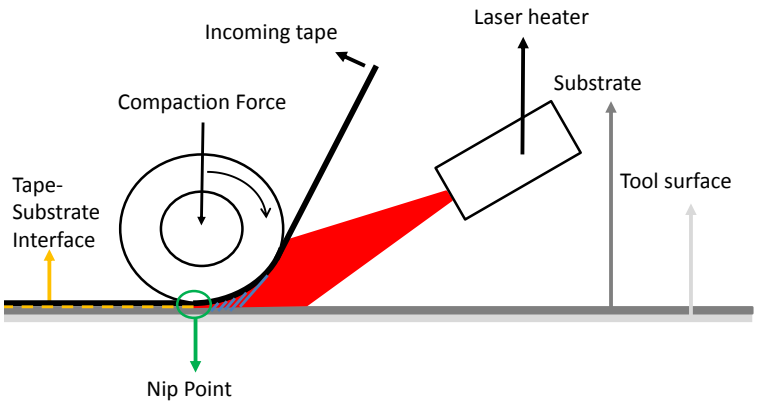

Figure 1. Laser assisted tape placement process

2.2 Material

Temperature dependent thermal properties for CF-PEEK which are available in the literature are used for a more accurate material behavior. The density, conductivity and the specific heat capacity of the material is summarized in Table 1.

Table 1. Temperature dependent thermal properties of CF-PEEK [3]

Temperature (°C)	Density (kg/m³)	Specific Heat (kJ/kg°C)	Thermal conductivity, Axial (W/m°C)	Thermal conductivity, Transverse (W/m°C)
0	1601	800	3.5	0.42
50	1598	930	4.6	0.52
100	1593	1040	5.1	0.6
150	1586	1260	5.9	0.7
200	1575	1300	5.9	0.7
250	1563	1400	6.1	0.7
300	1551	1550	6.7	0.75
350	1537	1650	6.8	0.68
400	1524	1700	7	0.65

2.3 Thermal Model

2.3.1 Heat Source Model

A uniform heat flux of 0.3 kW/mm^2 on an area 50x50 mm^2 is applied on both the tape and the substrate surfaces. The placement speed is set to 100 mm/s, so the heat flux moves on

the surfaces with that speed. Subroutine 'DFLUX' is used to implement the movement of the heat source.

2.3.2 Heat Transfer Within the Layers

The process model includes a 3-dimensional transient conduction equation described by the following expression:

$$\nabla(K\nabla \mathrm{T}) + \ddot{q} = \rho C\left(\frac{\partial T}{\partial t}\right)$$

Where K is the conductivity of the material, T is the temperature, $\ddot{q}$ is the volumetric heat generation, ρ is the density and C is the specific heat capacity of the material. Volumetric heat generation term in this equation refers to the energy released or absorbed during the melting or the crystallization phases of the polymer material. In this work, laser illumination is assumed to be the dominant heat input and the heat generation term is neglected. This assumption has been used by several authors [4–6].

2.3.3 Heat Loss to the Ambient Environment, Compaction Roller and the Mold

The heat loss to the air and the compaction roller from the top surface of the incoming tape is modelled by using the 'FILM' subroutine. A constant temperature of 25 °C and a convection coefficient of 10 W/m^2°C is used for heat loss to the ambient air. For the heat loss to the compaction roller, a convection coefficient of 400 W/m^2°C and a constant temperature of 25 °C is assumed. The convection coefficient for the roller moves with 100mm/s, on an area of 20x50 mm, 10 mm behind the zone heated by the heat source. Finally, the heat loss to the mold is modelled as a stationary convection coefficient of 400 W/m^2°C at the bottom surface of the substrate, assuming the contact of the composite and metal. These values are also present in the literature [3].

2.4 Degree of Intimate Contact

The degree of intimate contact represents the amount of flattening of the rough thermoplastic surfaces under the compaction roller. It is essential for bonding development between the layers and calculated by the following equation [7].

$$D_{ic} = \frac{1}{1+\frac{w_0}{b_0}}\left[\left(1+\frac{w_0}{b_0}\right)\left(\frac{a_0}{b_0}\right)^2 \int_0^{t_c} \frac{P_{app}}{\mu_{mf}}\,dt\right]^{\frac{1}{5}}$$

where the surface geometrical parameters $\frac{w_0}{b_0}$ is 1, $\frac{a_0}{b_0}$ is 0.3, the viscosity of the fiber resin mixture μ_{mf} is $1.14\cdot10^{-12}e^{26300/T}$. The viscosity is calculated using the average temperature of the tape and the substrate. P_{app} is taken as 0.2 MPa and modelled as a moving variable for nodes, occupying the same geometry with the convection coefficient for heat loss to the roller, which is explained in section 2.3.3. The integral term in the equation is calculated using the trapezoidal rule.

2.5 Analysis Domain and Deposition of the Layers

A 300-by-300 mm domain is considered for the analyses. 6.35 mm wide, 100 mm long pieces are partitioned at the center of each layer along the material/placement direction to act as the incoming tape. At the beginning of the analysis, the elements of the first incoming tape

are activated. The heat source and the compaction roller are moved on the tape, with the use of the subroutines mentioned above. After the deposition of the first tape is completed, the remaining elements in the 300-by-300 plate are activated to represent the substrate for the placement of the next tape. This procedure of placing the (n-1)th tape, activating the (n-1)th substrate and placing the nth tape continues until the desired laminate sequence is achieved. The process is shown in Figure 2.

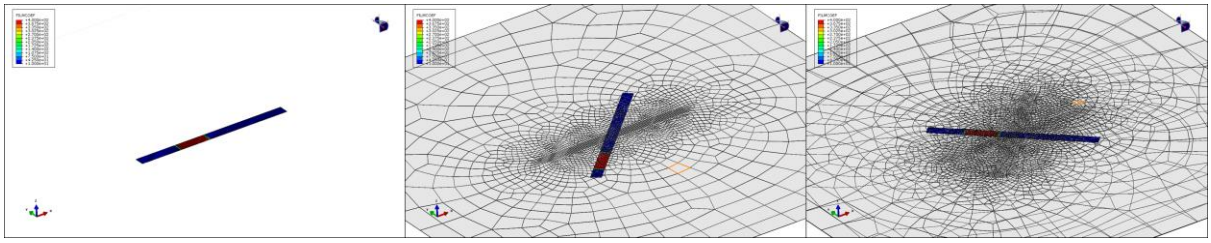

Figure 2. Deposition of 3 consecutive layers, showing the activation of substrate material after the tape is placed. Left to right: 0 degree, 45 degree and -45 degree.

3. METHODOLOGY

In order to show the effects of 3-dimensional analysis domain and the laminate sequence on temperature distribution, two different cases are analyzed. The first model is the manufacturing simulation of a $[0, 45, -45, 90]_S$ laminate with proper definitions of laser heater and roller convection movement. The second model consists of the same laminate sequence but assumes the motion of the laser heater and the roller in 0-direction for all of the layers regardless of the actual material orientation, with the purpose of imitating a 2-dimensional model. From now on, the models will be recalled as QI and QI-UD, respectively. The two cases are illustrated in Figure 3.

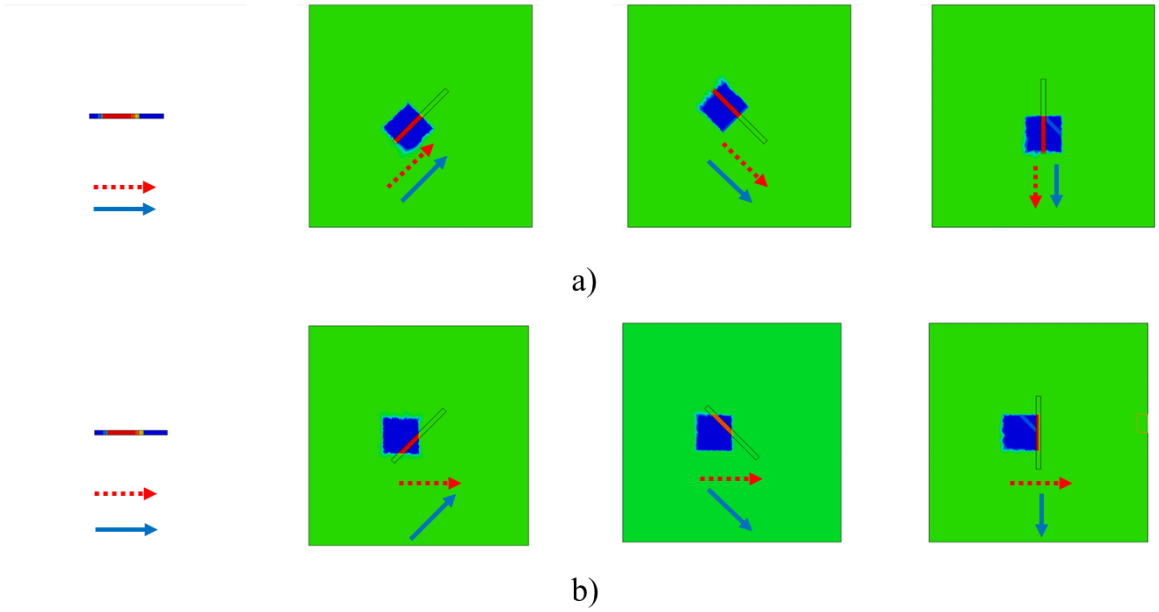

Figure 3. Material direction (blue arrow) and heat source movement direction (red dashed arrow) for the first 4 plies of $[0, 45, -45, 90]_S$ laminate. a) QI model b) QI-UD model

Temperature and degree of intimate contact history are extracted and averaged over the nodes at the intersection of the placed tapes. This intersection zone is shown in Figure 4.

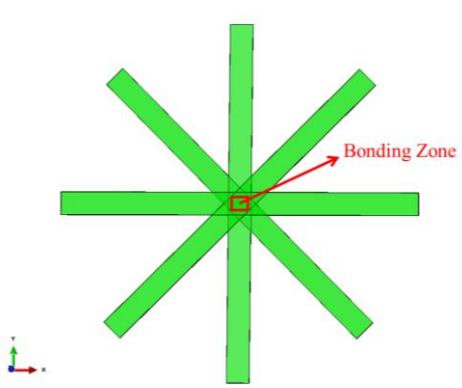

Figure 4. The partitioned geometries representing the incoming tape for each layer and the bonding zone over which the data for temperature and degree of intimate contact is averaged

4. RESULTS

Full thermal histories of the layers throughout the process are obtained. The temperature histories at the tape and the substrate are shown in Figure 5 and Figure 6, for both cases under consideration. The results of the thermal analysis show similar trends to the literature, as shown in previous work [8].

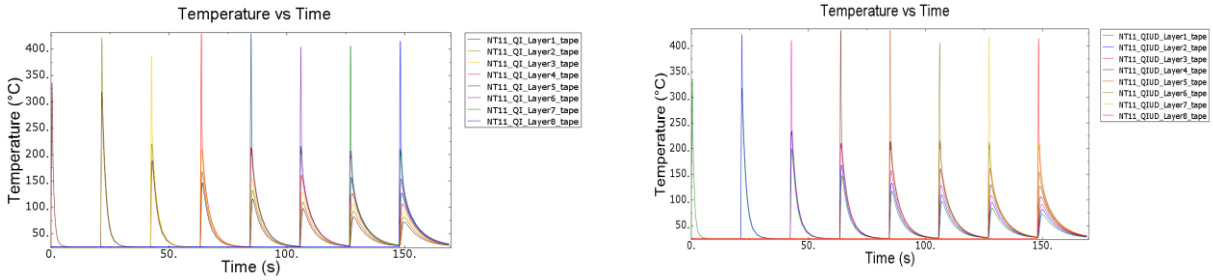

Figure 5. Averaged temperature histories over the bonding zone. Left: QI-tape surface, right: QI-UD-tape surface

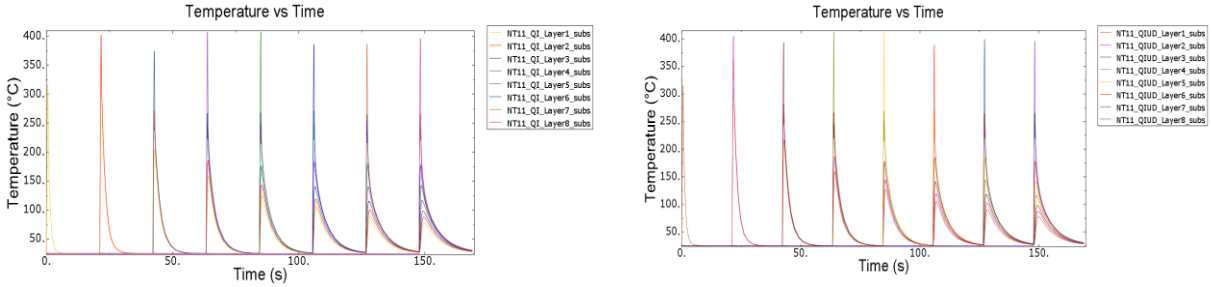

Figure 6. Averaged temperature histories over the bonding zone. Top: QI-substrate surface, bottom: QI-UD-substrate surface

4.1 Nip Point Temperatures

The temperature at the nip point has been the main interest for the majority of the thermal analyses of the LAFP process due to its direct link to the final quality of the part. In order to compare the effect of analyzing 3-dimensional heat source motion, nip point temperatures on the tape and substrate surfaces at each layer are extracted from the temperature histories presented above.

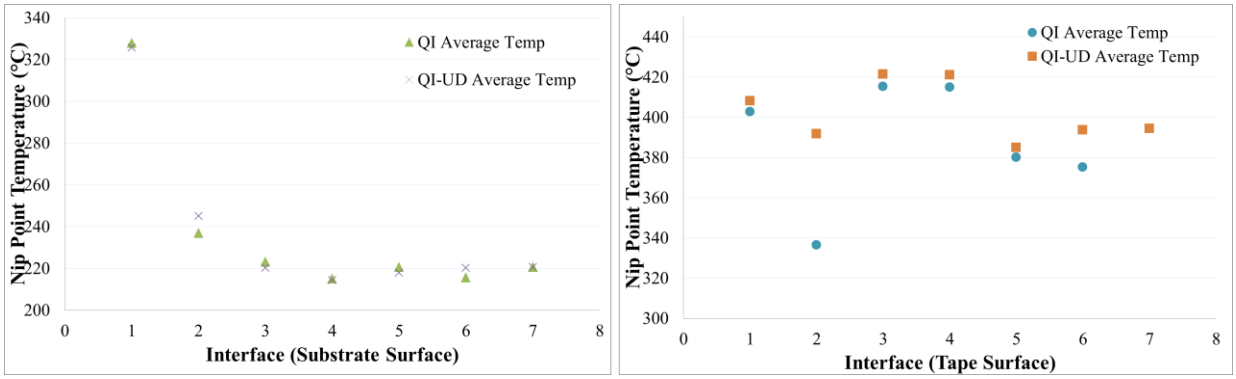

Figure 7. Nip point temperatures at each interface. Left: substrate surface, right: tape surface

Examining the nip point temperatures at each interface from Figure 7, a significant drop is observed at the 2nd and the 6th interfaces for both the tape and the substrate surfaces in the QI model when compared to the QI-UD model. The common point of these two interfaces is that the difference in fiber orientation between the incoming tape and the substrate is the most (i.e. 90°, between -45° and 45° layers). Temperature differences up to 16% are observed. The anisotropic thermal conductivity of the material affects the temperature distribution significantly in case of the maximum difference of fiber orientation between the tape and the topmost layer of the substrate. It is not possible to account for such effects in 2-dimensional thermal models.

4.2 Degree of Intimate Contact Evolution

Degree of intimate contact is calculated at each interface to show the effects of 3-dimensional modeling. Figure 8 shows the final degree of bonding at each interface. The results follow the same trend as the nip point temperatures, as expected. The largest difference between the models is observed at the 2nd and the 6th interfaces, which are between 45° and -45° plies. The QI-UD model overestimates the degree of bonding up to 14% at the interfaces where the fiber orientation difference between the tape and the substrate is maximum. A closer look on the intimate contact development at the 2nd and the 6th interfaces reveals that the difference between the two models occurs mainly at the first moment the layers are compacted, as it can be seen in Figure 9. The effect of subsequent passes on the change in degree of intimate contact diminishes.

5. CONCLUSIONS AND FUTURE WORK

In this work, validity of 2-D thermal models for LAFP of multiaxial laminates is investigated. Comparison of a 3-D thermal model with proper heat source movement and a model mimicking the 2-D thermal models showed that the nip point temperature and the

degree of bonding at the interfaces might be overestimated when the 2-D assumptions are used. This suggests that 2-dimensional models should be used with a precaution for multiaxial laminates.

A 3-dimensional transient finite element model for temperature and degree of intimate contact prediction for LAFP is presented within the context of this work. Such a model can be used to predict the final part quality for more complex design features which are likely to be used in the in situ consolidated parts in the near future. Experimental validation for temperature history and final degree of intimate contact is the next step to be taken.

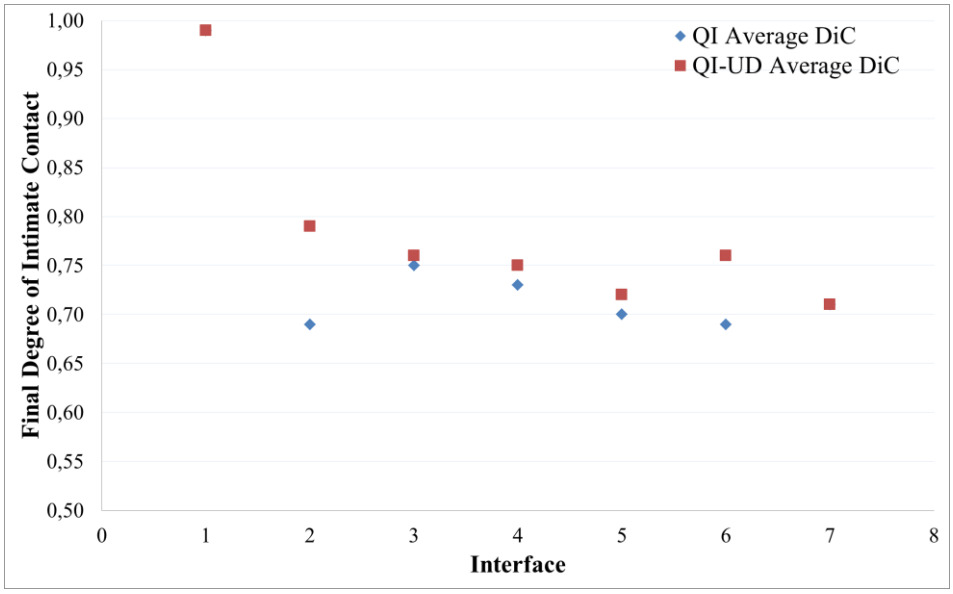

Figure 8. Final degree of intimate contact at each layer

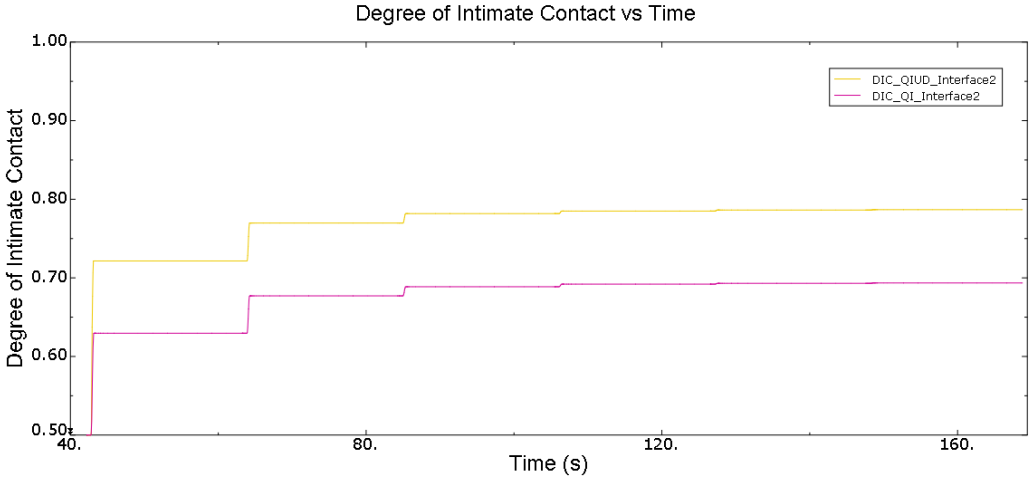

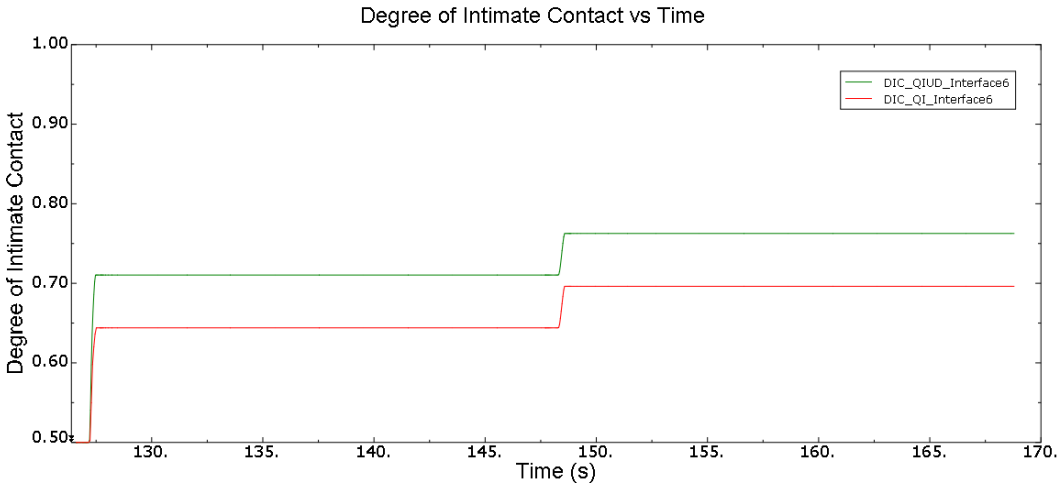

Figure 9. Degree of intimate contact evolution. Top: the 2nd interface, bottom: the 6th interface

6. ACKNOWLEDGMENTS

This work is funded by Netherlands Aerospace Center (NLR), within the project Smart Industry Fieldlab: ACM. The project is a part of the European Fund for Regional Development (EFRD), under the grant number KVW-00043.

7. REFERENCES

[1] W.M. van den Brink, R. Bruins, C.P. Groenendijk, P. Lantermans, R. Maas, Fibre Steered Skin Design of Composite Thermoplastic Horizontal Stabilizer Torsion Box. NLR-TP-2016-265, 2017.

[2] T. Orth, C. Weimer, M. Krahl, N. Modler, J. Plast. Technol. 11 (2015).

[3] F.N. Cogswell, Thermoplastic Aromatic Polymer Composites: A Study of the Structure, Processing, and Properties of Carbon Fibre Reinforced Polyetheretherketone and Related Materials, Butterworth-Heinemann, 1992.

[4] R. Pitchumani, S. Ranganathan, R.C. Don, J.W. Gillespie, M.A. Lamontia, Int. J. Heat Mass Transf. 39 (1996) 1883–1897.

[5] C.M. Stokes-Griffin, P. Compston, T.I. Matuszyk, M.J. Cardew-Hall, J. Thermoplast. Compos. Mater. 28 (2013) 1445–1462.

[6] J. Tierney, J.W. Gillespie, J. Compos. Mater. 37 (2003) 1745–1768.

[7] S.C. Mantell, G.S. Springer, J. Compos. Mater. 26 (1992) 2348–2377.

[8] G.K. Jeyakodi, S. Shroff, in:, Proc. Third Int. Symp. Autom. Compos. Manuf., Montreal, 2017.